Polydisperse star polymer solutions

C. von Ferber, A. Jusufi, M. Watzlawek,* C. N. Likos, and H. Löwen
Institut für Theoretische Physik II, Heinrich-Heine-Universität Düsseldorf, Universitätsstraße 1, D-40225 Düsseldorf, Germany

Abstract

We analyze the effect of polydispersity in the arm number on the effective interactions, structural correlations and the phase behavior of star polymers in a good solvent. The effective interaction potential between two star polymers with different arm numbers is derived using scaling theory. The resulting expression is tested against monomer-resolved molecular dynamics simulations. We find that the theoretical pair potential is in agreement with the simulation data in a much wider polydispersity range than other proposed potentials. We then use this pair potential as an input in a many-body theory to investigate polydispersity effects on the structural correlations and the phase diagram of dense star polymer solutions. In particular we find that a polydispersity of 10%, which is typical in experimental samples, does not significantly alter previous findings for the phase diagram of monodisperse solutions.
PACS 82.70.Dd, 64.60.Fr, 61.20.Ja, 61.41.+e

I. INTRODUCTION

A star polymer consists of linear polymer chains tethered to one common central core. The number of polymer chains f is usually referred to as *arm number* or *functionality*. If the degree of polymerization, i.e., the number of monomers per chain, N, is the same for all chains, the star polymer is called monodisperse with respect to N or "regular". For large N, the size of the central core particle is much smaller than the overall extension of the whole star. For a single star, the density of monomers around the central particle, $\phi(r)$, is radially symmetric, and from this density profile the so-called corona diameter σ, which measures the extension of the star, can be defined as the diameter of a sphere around the star center where all Nf monomers are found "inside" [1].

In the last years, star-shaped polymer aggregates have attracted a considerable amount of interest from both the experimental and the theoretical point of view [2–4]. The reason for that is threefold. First, from a technical point of view, star polymers are important for several industrial applications [2]. One example are hydrogenated polyisoprene star polymers, which are used as viscosity index modifiers in oil industry applications due to their

*Present address: Bayer AG, Central Research Division, D-51368 Leverkusen, Germany

excellent shear stability. Further, commercial star polymers are brought into action in coating materials, as binders in toners for copying machines, and in several pharmaceutical and medical applications [2]. Second, from an experimental point of view, the recent synthesis of regular star polymers with various possible numbers of arms by Roovers and coworkers [5,6] made it possible to explore the physics of well-defined model systems, which are monodisperse in both the number of arms and the degree of polymerization. Important examples are polyisoprene stars with $f = 8, 18$ [7] and polybutadiene stars with $f = 32, 64, 128$ [6], both synthesized by anionic polymerization. Third, star polymers constitute an important soft-condensed matter system, linking the fields of polymer physics and colloid physics, thus attracting also interest from a purely theoretical point of view. Star polymers with small arm numbers ($f = 1, 2$) resemble linear polymers. Thus, their configurations show a considerable asphericity [8–10], although their chain-averaged number density of monomers, $\phi(r)$, is spherically symmetric around the center of mass of the polymer. With increasing arm number f, the asphericity of the stars has been shown to decrease considerably [11–19], leading to "stiff" spherical particles in the limit of high f. It is essentially this limit that a description of star polymers as sterically stabilized colloidal particles holds. This polymer-colloid hybrid character of star polymers has been explored in a number of publications dealing with the structural [2,7,20–32] and dynamical [23–25,33–38] properties of star polymers.

In the usual theoretical description, star polymers in dense solution are considered as an effective one-component (monodisperse) system, i.e., all the stars have the same arm number f and all the linear polymer chains attached to the center have the same molecular weight. While the latter can be realized by a careful preparation method, the former is in general not true in actual samples. The preparation of star polymers proceeds by adding linear polymer chains to a dendrimer-like core with reactions centers placed at the end of the dendrimer and the polymer chains. The chemical reaction is typically incomplete such that few of the reaction centers at the dendrimer are not linked to a linear chain. Hence an intrinsic polydispersity in the arm number arises. By ultracentrifugation one can estimate the relative polydispersity in the arm number to be around 5-15 percent in carefully and slowly prepared samples. It can, however, also be much larger for fast reactions [39,40]. In a comparison between experimental data and theory, in almost all previous studies the assumptions of a monodisperse sample was implicitly made such that a natural question concerns the influence of polydispersity on the statistical properties of star polymer solutions. As far as theory is concerned, the situation resembles much the case of colloidal suspensions where the effect of charge and size polydispersity has been a topic of intense recent research, see Refs. [41–46] for recent reviews.

In this paper, we investigate the effect of arm number polydispersity on the effective interaction, the structural correlations and the phase diagram for star polymer solutions in a good solvent. Our work is based on a theoretical analysis using scaling theory and computer simulations. We first derive the effective interaction between two star polymers of different arm numbers f_1 and f_2 from scaling assumptions. Basically the interaction is logarithmic with the core-core distance r between the two stars but the prefactor depends explicitly on f_1 and f_2 and differs from that of a monodisperse sample. The resulting pair potential is tested against molecular simulations and good agreement is found even when f_1 is very different from f_2 while earlier descriptions [47] are found to hold for small polydispersities but to be too simplistic for large polydispersities. In a further step towards a full description of dense

star polymer solutions, we then perform computer simulations of a classical many-body systems interacting by means of this effective pair interaction. We find that a polydispersity in the arm number reduces the structural correlations but this effect is less drastic than for size polydispersity in sterically stabilized colloidal suspensions. Further, we present evidence that the reentrant melting behavior predicted from the theoretical treatment of a monodisperse description [21,30,31,48] does not change drastically in a polydisperse solution of star polymers.

The paper is organized as follows: In section II we present the scaling ideas and derive the effective interaction potential between two stars of different arm numbers. A test of this result against molecular computer simulation is performed in section III. Results for the structure and phase diagram from a simulation of a many-body system are given in section IV. Finally, we conclude in section V.

II. SCALING THEORY FOR AN EFFECTIVE POTENTIAL

The effective interaction between two star polymers results from the steric interaction of all monomers that constitute the polymer chains on each of the stars. It is obviously a formidable task to derive the effective potential from first principles. Luckily we are in the position to give a rigorous result for the limiting case of short distance between the two star cores, while good arguments exist for the description of the long range part of the interaction. We have found in the treatment of the interaction of monodisperse star polymers that the combination of these two approaches leads to good agreement with simulation results as well as with scattering experiments on real star polymer systems [28,49,50].

We first derive the short distance interaction using scaling arguments. Many details of the behavior of polymer solutions may be derived using the renormalization group (RG) analysis [51]. Here, we use only the more basic results of power law scaling: the radius of gyration $R_1(N)$ of a single linear polymer chain with N monomers and its partition function $\mathcal{Z}_1(N)$ are found to obey the power laws:

$$R_1(N) \sim N^{\nu} \qquad \text{and} \qquad \mathcal{Z}_1(N) \sim z^N N^{-\nu\eta_2} \,. \tag{1}$$

The fugacity z measures the mean number of possibilities to add one monomer to the chain. It is microscopic in nature and will depend on the details of the theoretical model or the experimental system. The two exponents ν and η_2 on the contrary are universal to all polymer systems in a good solvent, i.e., excluding high concentration of polymers or systems in which the polymers are collapsed or are near the collapse transition. A family of additional exponents η_f governs the scaling of the partition functions $\mathcal{Z}_f(N)$ of polymer stars of f chains each with N monomers while the power law for the radius of gyration remains unchanged:

$$R_f(N) \sim N^{\nu} \qquad \text{and} \qquad \mathcal{Z}_f(N) \sim z^{fN} N^{\nu(\eta_f - f\eta_2)}. \tag{2}$$

The exponents of any other power law for more general polymer networks are given by scaling relations in terms of η_f and ν [52–54]. Note that eqs. (1) and (2) imply $\eta_1 = 0$. The values of these exponents are known from RG and Monte Carlo (MC) simulations [55]. In the limiting case of many arms, $f \gg 1$, the leading behavior of η_f is given by [56]

$$\eta_f \sim -f^{3/2}, \tag{3}$$

a result that has been found also from of geometrical considerations using the blob model of a star polymer [20]. The scaling law for the partition sum of two star polymers may be derived from a short distance expansion [57,58]. The partition sum of the two stars $\mathcal{Z}_{f_1 f_2}(N, r)$ at small center-to-center distances r factorizes into a function $C_{f_1 f_2}(r)$ and the partition function $\mathcal{Z}_{f_1+f_2}(N)$ of the star with $f_1 + f_2$ arms that is formed when the cores of the two stars coincide:

$$\mathcal{Z}_{f_1 f_2}(N, r) \sim C_{f_1 f_2}(r) \mathcal{Z}_{f_1+f_2}(N)\,. \tag{4}$$

Such a behavior is generally assumed in scaling arguments . At large star-star separation $\mathcal{Z}_{f_1 f_2}(N, r)$ is the product of the single star partition functions. Again we may argue that the ratio of the partition function of two stars at finite separation r to that at infinite separation can only be a function B of r/R_1 noting that R_1 is the only relevant length scale in this problem (R_{f_1} and R_{f_2} differ from R_1 only in an f-dependent prefactor):

$$\mathcal{Z}_{f_1 f_2}(N, r) \sim B_{f_1 f_2}(r/R_1) \mathcal{Z}_{f_1} \mathcal{Z}_{f_2}\,. \tag{5}$$

Taking this into account and inserting the power law scaling according to Eqs. (1) and (2) we find that Eqs. (4) and (5) are only compatible if also $C(r)$ follows a power law

$$C_{f_1 f_2}(r) \sim r^{\Theta^{(\mathrm{s})}_{f_1 f_2}}\,, \tag{6}$$

and the so-called contact exponent $\Theta^{(\mathrm{s})}_{f_1 f_2}$ obeys the scaling relation

$$\Theta^{(\mathrm{s})}_{f_1 f_2} = \eta_{f_1} + \eta_{f_2} - \eta_{f_1+f_2}\,. \tag{7}$$

Note that in terms of the RG of polymer field theory the exponents η_f correspond to dimensions of operators associated with the partition functions of single stars [54] and relation (7) is a direct consequence of the short distance expansion. The mean force $F_{f_1 f_2}(r)$ acting on the centers of two star polymers with f_1 and f_2 arms is now derived as the gradient of the effective potential $V^{\mathrm{eff}}(r) = -k_{\mathrm{B}}T \log[\mathcal{Z}_{f_1 f_2}(r)/(\mathcal{Z}_{f_1} \mathcal{Z}_{f_2})]$ with $k_{\mathrm{B}}T$ denoting the thermal energy. For the force at short distances r this evidently results in

$$F_{f_1 f_2}(r) = k_{\mathrm{B}}T \frac{\Theta^{(\mathrm{s})}_{f_1 f_2}}{r}\,. \tag{8}$$

Using the above many arm limit for η_f one may match the contact exponents $\Theta^{(\mathrm{s})}_{ff}$ to the known values for $f = 1, 2$ [59] fixing the otherwise unknown prefactor in eq. (3). Assuming that the behavior of the $\Theta^{(\mathrm{s})}_{ff}$ may be described by this approximation for all f one finds:

$$F_{ff}(r) \approx k_{\mathrm{B}}T \frac{5}{18} \frac{f^{3/2}}{r}\,. \tag{9}$$

This matching in turn suggests an approximate value for the η_f exponents, taking into account $\eta_1 = 0$ and $\eta_2 \approx -5/18$:

$$\eta_f \approx -\frac{5}{36}\frac{f^{3/2}-f}{\sqrt{2}-1}\,. \tag{10}$$

Inserting this into the general formula for the interaction of two different star polymers the contact exponent reads for large f_1 and f_2

$$\Theta^{(\mathrm{s})}_{f_1 f_2} = \frac{5}{36}\frac{1}{\sqrt{2}-1}\left[(f_1+f_2)^{3/2} - \left(f_1^{3/2}+f_2^{3/2}\right)\right]. \tag{11}$$

We note that on a phenomenological level there are other possibilities to describe the interaction in a polydisperse system of star polymers. In colloidal systems two other approaches to the interaction of polydisperse particles are commonly used: in a steric stabilized system with a polydispersity in the radii of the particles one expects to find an interaction radius that is the *arithmetic mean* of the radii of the two interacting particles [44,60]. In a charge stabilized solution the other hand, the interaction of two particles is proportional to the product of the two charges and the effective charge is calculated as the *geometric mean* of the two charges. The latter description was used in an earlier investigation of star polymers treating f as an "effective charge" parameter [47,61,62]. For comparison with these other possible approaches we define:

$$\Theta^{(\mathrm{a})}_{f_1 f_2}(r) = \frac{5}{18}\left(\frac{f_1+f_2}{2}\right)^{3/2}\,, \tag{12}$$

$$\Theta^{(\mathrm{g})}_{f_1 f_2}(r) = \frac{5}{18}\left(\sqrt{f_1 f_2}\right)^{3/2}\,. \tag{13}$$

We now turn to the interaction at larger separation. It has been recently shown that a Yukawa like tail for the potential between star polymers reproduces the results of both simulation and scattering experiments for monodisperse solutions [28,49,50]. The natural scale for a star polymer is the corona diameter $\sigma_f = 2\lambda R_f$ with $\lambda \approx 2/3$ [49]. For the potential between two f-arm star polymers at distance $r > \sigma_f$ one has

$$V_{ff}(r) \sim \frac{1}{r}\exp(-r\kappa_f). \tag{14}$$

The decay length $1/\kappa_f = 2\sigma_f/\sqrt{f}$ is the diameter of the outermost blobs of the star polymer in the Daoud-Cotton model [1,28].

In a simple but successful approach the full potential for the interaction between two f-arm star polymers was constructed by concatenating the long range and short range potentials. In this model the crossover from short to long range behavior takes place when the distance of the two cores is σ_f. It is natural to generalize this to two star polymers with f_1 and f_2 arms in such a way that the crossover point is at distance $\sigma = (\sigma_{f_1} + \sigma_{f_2})/2$. It is less obvious how to choose the decay length of the long range part. Our choice $1/\kappa = 1/\kappa_{f_1} + 1/\kappa_{f_2}$ is in accordance to the simulation results presented below. Note that although we have omitted the subscripts on σ and κ, the latter are functions of f_1 and f_2.

The full potential then reads

$$\frac{1}{k_{\rm B}T}V_{f_1f_2}(r) = \Theta^{(\rm s)}_{f_1f_2} \begin{cases} -\ln(\frac{r}{\sigma}) + \frac{1}{1+\sigma\kappa} & \text{for } r \le \sigma; \\ \frac{1}{1+\sigma\kappa}\frac{\sigma}{r}\exp(\sigma\kappa - r\kappa) & \text{for } r > \sigma. \end{cases} \tag{15}$$

In the monodisperse case $f_1 = f_2$ this potential reduces to the one between two identical star polymers that has been successfully tested in extensive simulations.

III. COMPARISON WITH SIMULATION RESULTS

We have performed Molecular Dynamics (MD) computer simulations of two star polymers with different arm numbers f_1 and f_2 by resolving the monomers as classical beads along the chains. We use the same simulation model as in previous studies of star polymer solutions in a good solvent [49,63]. The arm length, i.e., the number N of beads along each chain, was kept fixed to $N = 50, 100$ which was shown in previous work to be large enough to guarantee a sufficient scaling behavior. The main features of the simulation model can be summarized as follows:

1. A purely repulsive truncated Lennard-Jones interaction between all $N(f_1 + f_2)$ monomers is assumed.

2. An attractive FENE-potential is added for the interaction between neighboring monomers along a chain.

3. To accommodate the polymer arms, a hard core with radius $R^{(d)}$ is introduced at the center of the stars. The cores interact with the monomers according to the above mentioned potentials with a separation shift of $R^{(d)}$.

Two stars with arm numbers f_1 and f_2 were fixed at core separation r. After a long equilibration period, the total force $F_{f_1f_2}$ acting onto the cores is averaged. The temperature T is kept constant. Both the equilibration time and the time during which averages were performed was about 1000τ where $\tau = \sqrt{m\sigma^2/\epsilon}$ is the Lennard-Jones time unit with σ, ϵ and m denoting the Lennard-Jones length, energy scale and the monomer mass. A simulation snapshot is shown in Fig. 1. When comparing the mean force to the derivative of the theoretical effective potential, two technical problems arise: (i) In contrast to the theory, we have a finite core size $R^{(d)}$ which is the same for both stars. (ii) The two corona diameters, σ_f, $(f = f_1, f_2)$ which enter in the potential of eq. (15), are not directly accessible in a simulation.

As in the monodisperse case [49], the first difficulty (i) is overcome by plotting the inverse force $1/F_{f_1f_2}$ versus distance r. The divergence in the force occurs already at core separations $r \cong 2R^{(d)}$ which leads to a zero in the $1/F_{f_1f_2}$ plot. The inverse *slope* of the $1/F_{f_1f_2}$-plot then corresponds to the prefactor $\Theta^{(s)}_{f_1f_2}$ of the logarithmic term in the effective pair potential. It is this slope which can directly be compared to our theoretical prediction eq. (15). Furthermore, a linear function in the $1/F_{f_1f_2}$ plot is a direct check for the validity of the $\ln r$-term in the effective interaction potential, eq. (15).

To handle the second difficulty (ii) we consider the radius of gyration R_f of each star which is readily accessible in a simulation of a single star [49]. We assume a proportionality between the R_f and σ_f,

$$\sigma_f = 2\lambda R_f \tag{16}$$

and use λ as a fit parameter to fit the full force versus distance curve for given arm numbers f_1 and f_2. The results for the optimal fit parameter are shown in Table I. We obtain an averaged value of $\langle\lambda\rangle \approx 0.66$, which is nearly independent of f_1, f_2. Thus, the results found here are consistent with those from the previously investigated monodisperse case [49]. We further remark that this value coincides with that used in Ref. [28] to fit experimental data for $f = 18$ and that λ is independent of N, consistent with scaling theory.

Results for the comparison between theory and simulation are shown in Figure 2 where the reduced inverse mean force $1/F_{f_1 f_2}$ between the star centers is plotted versus intercore distance r for two arm numbers $f_1 = 10$ and $f_2 = 50$. We observe two important facts: first, the data indeed fall on a straight line proving the logarithmic behavior of the potential inside the mean corona. The straight line hits the origin at $r = 2R^{(d)}$ showing the relevance of the finite core in the simulations. Second, the inverse slope $\Theta_{f_1 f_2}$ agrees very well with the theoretical prediction also shown in Figure 2. A similar behavior was observed for all other combinations of arm numbers contained in Table I.

In Fig. 3, the prefactor $\Theta_{f_1 f_2}$ is plotted versus f_2, at a fixed value $f_1 = 10$, and compared to the different theoretical predictions in eqs. (11)-(13). Of course, in the monodisperse case $f_1 = f_2 = 10$, all the different theoretical expressions for $\Theta_{f_1 f_2}$ coincide and agree well with the simulation, consistently with our earlier work [49]. For increasing asymmetry between f_1 and f_2, significant deviations between the predictions of (a) an arithmetic or (g) a geometric mean and the simulation results become visible. While the expression $\Theta^{(s)}_{f_1 f_2}$ gained from scaling theory is able to describe the slope even for large asymmetries, $\Theta^{(g)}_{f_1 f_2}$ is worse at large asymmetries while $\Theta^{(a)}_{f_1 f_2}$ even possesses the wrong curvature as a function of f_2. Similar conclusions hold for other combinations of f_1 and f_2.

In Fig. 4, we show the force $F_{f_1 f_2}$ versus distance $r - R^{(d)}$, scaled by $R_{12} = (R_{f_1} + R_{f_2})/2$, comparing the theoretical force with simulation results for three cases: $f_1 = 10, 18, 30; f_2 = 50; N = 50$. Note that formally the core size $R^{(d)}$ vanishes in the theory. There is a good overall agreement inside the corona region between theory and simulation even for large asymmetries of f_1 and f_2. Results for distances r outside the corona, $r > \sigma$, are presented in Figure 5. Here, we test the exponential decay of the force $F_{f_1 f_2}$ with distance r by plotting the logarithm of the force versus distance. The crossover of the inner-core data to a straight line outside the core is clearly visible. Within the simulation error bars, the slope is consistent with the theoretical prediction eq. (15).

IV. POLYDISPERSITY EFFECTS IN DENSE STAR POLYMER SOLUTIONS

To explore the effects of arm number polydispersity on the structure and phase behavior of dense solutions of star polymers, we further performed large scale Monte Carlo simulations using the pair potential approach as given by the potential in eq. (15). Thus, on the one hand, this approach closely corresponds to our recent work on the structural and phase behavior of monodisperse star polymer solutions [29–31], and, on the other side, is quite similar to investigations of polydispersity effects in solutions of hard spheres [44,60,64,65] and charged colloidal particles [45,61,62,66] available in the literature.

In our MC simulations, representative particle configurations of approximately 2000 star polymers in a cubic simulation box were created in the following manner. First, a starting particle configuration was built up by placing the particles on random positions in the box, each particle assigned with an arm number f chosen from a Gaussian distribution $g(f)$ of mean $\bar{f}$ and variance $p = \sqrt{\overline{f^2} - \bar{f}^2}$:

$$g(f) = \frac{2}{p\sqrt{2\pi}} \exp\left[-\frac{1}{2p^2}\left(f - \bar{f}\right)^2\right]. \tag{17}$$

We use eq. (17) above to *define* the polydispersity p in what follows. The Gaussian distribution chosen to describe arm number polydispersity agrees well with experimentally-determined arm number distributions of star polymers synthesized by anionic polymerization [50]. Note that nonphysical, negative arm numbers, which are in principle not prohibited by a Gaussian arm number distribution, did not occur in the simulations for the values of $\bar{f}$ and p chosen here. Second, an equilibration phase of approximately 50 000 MC cycles was performed by allowing both translational particle moves according to the standard Metropolis scheme, and particle exchanges of randomly chosen particle pairs, again using the Metropolis rule to decide an exchange to happen or not. For the calculation of pair potential energies, eq. (15) was used, together with the scaling relation [1]:

$$\frac{\sigma_{f_1}}{\sigma_{f_2}} = \left(\frac{f_1}{f_2}\right)^{1/5}. \tag{18}$$

After the equilibration phase, approximately 100 000 MC cycles were simulated to gather statistics for both the radial center-to-center distribution function $g(r)$ and the center-to-center structure factor $S(k)$ [41,42,44,45,67]. In what follows, we will use $\bar{\sigma} = \sigma_{\bar{f}}$ as the basic length scale, and the mean packing fraction $\bar{\eta} = \rho\bar{\sigma}^3\pi/6$ (ρ being the number density of the stars) as a measure of the density.

In order to investigate the polydispersity effects on the liquid structure of dense star polymer solutions, simulations with varying polydispersities p were performed at (average) arm numbers $\bar{f}$ and mean packing fractions $\bar{\eta}$, known to correspond to the liquid state in the monodisperse case $p = 0$ [30,31]. We show typical results for $g(r)$ and $S(k)$ in fig. 6. As can be seen, increasing the polydispersity leads to decreasing spatial correlations in the fluid, indicated by a decreasing principal peak height of both $g(r)$ and $S(k)$. Thus, as expected, the effect of arm number polydispersity in star polymer solutions is quite similar to the effect of charge polydispersity in solutions of charged colloids [45,66]. Note that the anomalous behavior of $S(k)$ reported for monodisperse star polymer solutions in Ref. [29] also holds for polydisperse star polymer solution for all polydispersities $p \leq 14$ simulated.

In order to explore the evolution of the freezing and reentrant melting phase transitions found for monodisperse star polymer solutions [30,31] with increasing polydispersity, we employed the following strategy. We performed a number of simulations at state points corresponding to the solid phase in the monodisperse case, gradually increasing the parameter p. In particular, we chose $\bar{f} = 40$ and $\bar{\eta} = 0.5$ in a first set of simulations. Our results for $g(r)$ and $S(k)$ are given in Fig. 7. Let us begin with the discussion of the $g(r)$-data. As the monodisperse case $p = 0$ corresponds to an solid state of bcc-symmetry [30,31], the shown $g(r)$ is, in fact, the radially-averaged pair correlation function of the stars in the

crystal state.[1] Again, increasing p leads to decreasing structural correlations between the particles indicated by a decreasing principal peak height and a "smearing-out" of the sub peak-structure of $g(r)$ seen for $p = 0$. This scenario also manifests itself in the structure factors shown in fig. 7(b). Notice that the corresponding structure factor for $p = 0$ exhibits strong Bragg peaks, again indicating the monodisperse system to be in the crystal state for $\bar{f} = f = 40$, $\bar{\eta} = \eta = 0.5$, and is not depicted for that reason. For nonzero polydispersities the simulated structure factors do not show Bragg peaks and the value of the principal peak heights $S_{\max}$ decreases. Thus, increasing the polydispersity in a sample of star polymers at $\bar{f} = f = 40$, $\bar{\eta} = \eta = 0.5$ leads to a melting transition from a *bcc* crystal to a fluid phase. We therefore expect polydisperse star polymer solutions to show an enlarged fluid phase region as compared to the phase diagram of monodisperse star polymers in Refs. [30,31]. Furthermore, the stability range of the fluid phase is expected to increase with increasing the polydispersity p. To corroborate this expectation in more detail, we have performed further MC simulations of polydisperse star polymers for various state points $(\bar{f}, \bar{\eta})$, all corresponding to state points close to the freezing or reentrant melting line in the monodisperse case [30,31]. For the ranges of polydispersity examined here, $(p \leq 14)$, no change in the topology of the phase diagram and no new crystalline phases were found as a result of polydispersity. A quantitative calculation of the full phase diagram by more sophisticated simulation methods [64,65] is beyond the scope of this paper and will be left for future studies.

V. CONCLUSIONS

In conclusion, we have analyzed the effect of arm number polydispersity on the effective interaction and the structural correlations between star polymers in a good solvent. An analytical expression for an effective pair potential, given by eq. (15), was put forward and its validity was confirmed by Molecular Dynamics computer simulation. This pair potential was subsequently used to simulate the structural correlations between many stars. As expected, correlations decrease with increasing polydispersity. At the same time, though, the effect is much less pronounced than for size-polydisperse hard spheres. This can be seen in analogy to colloidal suspensions where size polydispersity of sterically-stabilized suspensions is known to lead to much more pronounced effects than charge-polydispersity in charged suspension. The microscopic reason for that is that the effective interaction is much softer for charged colloids which is similar to our case of star polymers.

We finish with a couple of remarks: first it would be interesting to compare, both qualitatively and quantitatively, our theoretical predictions to experimental data. In fact, the intrinsic polydispersity in the arm number can be measured and structural correlations are accessible, e.g., by neutron scattering of a star polymer solution with marked cores. Second, it would be interesting to map out, for a given polydispersity, the full phase diagram including freezing into different solid structures. Also, it would be interesting to develop and

[1] In fact, from the typical particle-particle distances read off from the pair correlation function, it can be concluded that the crystal structure is bcc, a result which is in agreement with calculations of bond order correlation functions [31].

apply a liquid integral equation theory to predict structural correlations in a polydisperse star polymer solutions. The output of such a theory could be checked against our computer simulation data of section IV. Third, we have not considered a polydispersity in the length of the linear polymer chains attached to the centers. It would be interesting to study this theoretically and compare the results to samples prepared in such a way that different linear chains are brought to the reaction centers of the dendrimers. Work along these lines is left for future studies.

ACKNOWLEDGMENTS

This work has been supported in part by the SFB 237 of the Deutsche Forschungsgemeinschaft.

REFERENCES

[1] M. Daoud and J. P. Cotton, J. Physique **43**, 531 (1982).
[2] G. S. Grest, L. J. Fetters, J. S. Huang, and D. Richter, Adv. Chem. Phys. **XCIV**, 67 (1996).
[3] W. Burchard, Adv. Polym. Sci. **143**, 113 (1999).
[4] J. J. Freire, Adv. Polym. Sci. **143**, 35 (1999).
[5] L.-L. Zhou and J. Roovers, Macromolecules **26**, 963 (1993).
[6] J. Roovers *et al.*, Macromolecules **26**, 4324 (1993).
[7] W. D. Dozier, J. S. Huang, and L. J. Fetters, Macromolecules **24**, 2810 (1991).
[8] K. Solc and W. H. Stockmayer, J. Chem. Phys. **54**, 2756 (1971).
[9] K. Solc, J. Chem. Phys. **55**, 2335 (1971).
[10] G. Tanaka and W. L. Mattice, Macromol. Theory Simul. **5**, 499 (1996).
[11] K. Solc, Macromolecules **6**, 378 (1973).
[12] K. Solc, Macromolecules **13**, 506 (1980).
[13] J. Batoulis and K. Kremer, Macromolecules **22**, 4277 (1989).
[14] O. Jagodzinski, J. Phys. A **27**, 1471 (1994).
[15] G. Zifferer, J. Chem. Phys. **102**, 3720 (1995).
[16] G. Zifferer, Macromol. Theory Simul. **6**, 381 (1997).
[17] G. Zifferer, J. Chem. Phys. **110**, 4668 (1999).
[18] A. Forni, F. Ganazzoli, and M. Vacatello, Macromolecules **30**, 4737 (1997).
[19] A. Sikorski and P. Romiszowski, J. Chem. Phys. **109**, 6169 (1998).
[20] T. A. Witten, P. A. Pincus, and M. E. Cates, Europhys. Lett. **2**, 137 (1986).
[21] T. A. Witten and P. A. Pincus, Macromolecules **19**, 2509 (1986).
[22] D. Richter *et al.*, J. Physique IV **3**, 3 (1993).
[23] J. Roovers, Macromol. Symp. **121**, 89 (1997).
[24] M. Adam, L. J. Fetters, W. W. Graessley, and T. A. Witten, Macromolecules **25**, 2434 (1991).
[25] A. P. Gast, Langmuir **12**, 4060 (1996).
[26] L. Willner *et al.*, Europhys. Lett. **19**, 297 (1992).
[27] L. Willner *et al.*, Macromolecules **27**, 3821 (1994).
[28] C. N. Likos *et al.*, Phys. Rev. Lett. **80**, 4450 (1998).
[29] M. Watzlawek, H. Löwen, and C. N. Likos, J. Phys.: Condens. Matter **10**, 8189 (1998).
[30] M. Watzlawek, C. N. Likos, and H. Löwen, Phys. Rev. Lett. **82**, 5289 (1999).
[31] M. Watzlawek, *Phase Behavior of Star Polymers* (Shaker-Verlag, Aachen, 2000).
[32] C. von Ferber *et al.*, Eur. Phys. J. E **2**, 311 (2000).
[33] J. Roovers, Macromolecules **27**, 5359 (1994).
[34] R. Seghrouchni *et al.*, Europhys. Lett. **42**, 271 (1998).
[35] J. Stellbrink, J. Allgaier, and D. Richter, Phys. Rev. E **56**, R3772 (1997).
[36] D. Vlassopoulos *et al.*, Europhys. Lett. **39**, 617 (1997).
[37] P. A. Nommensen *et al.*, Progr. Coll. Polym. Sci. **110**, 144 (1998).
[38] G. Fleischer *et al.*, Physica A **280**, 266 (2000).
[39] K. Ishizu, T. Ono, and S. Uchida, J. Colloid Interface Science **192**, 189 (1997).
[40] S. Uchida, A. Ichimura, and K. Ishizu, J. Colloid Interface Science **203**, 153 (1998).
[41] P. N. Pusey, in *Liquids, Freezing and the Glass Transition*, edited by J. P. Hansen, D. Levesque, and J. Zinn-Justin (North Holland, Amsterdam, 1991).

[42] B. D'Aguanno and R. Klein, J. Chem. Soc. Faraday Trans. **87**, 379 (1991).
[43] P. Salgi and R. Rajagopalan, Advances in Colloid and Interface Science **43**, 169 (1993).
[44] H. Löwen, Phys. Rep. **237**, 249 (1994).
[45] G. Nägele, Phys. Rep. **272**, 215 (1996).
[46] J. K. G. Dhont, *An Introduction to Dynamics of Colloids* (Elsevier, Amsterdam, 1996).
[47] E. Lomba, private communication.
[48] G. A. McConnell and A. P. Gast, Macromolecules **30**, 435 (1997).
[49] A. Jusufi, M. Watzlawek, and H. Löwen, Macromolecules **32**, 4470 (1999).
[50] J. Stellbrink *et al.*, Progr. Coll. Polym. Sci. **115**, 88 (2000).
[51] L. Schäfer, *Excluded Volume Effects in Polymer Solutions as Explained by the Renormalization Group* (Springer, Berlin, 1999).
[52] B. Duplantier, Phys. Rev. Lett. **57**, 941 (1986).
[53] K. Ohno and K. Binder, J. Phys. (Paris) **49**, 1329 (1988).
[54] L. Schäfer, C. von Ferber, U. Lehr, and B. Duplantier, Nucl. Phys. B **374**, 473 (1992).
[55] J. Batoulis and K. Kremer, Macromolecules **22**, 4277 (1989).
[56] K. Ohno, Phys. Rev. A **40**, 1524 (1989).
[57] B. Duplantier, J. Stat. Phys. **54**, 581 (1989).
[58] C. von Ferber, Nucl. Phys. B **490**, 511 (1997).
[59] J. des Cloizeaux, J. Phys. (Paris) **36**, 281 (1975).
[60] J.-L. Barrat and J.-P. Hansen, J. Physique (Paris) **47**, 1547 (1986).
[61] B. D'Aguanno and R. Klein, Phys. Rev. A **46**, 7652 (1992).
[62] E. Allahyarov, H. Löwen, and S. Trigger, Phys. Rev. E **57**, 5818 (1998).
[63] G. S. Grest, K. Kremer, and T. A. Witten, Macromolecules **20**, 1376 (1987).
[64] P. G. Bolhuis and D. A. Kofke, J. Phys.: Condens. Matter **8**, 9627 (1996).
[65] P. G. Bolhuis and D. A. Kofke, Phys. Rev. E **54**, 634 (1996).
[66] R. Klein and B. D'Aguanno, in *Light Scattering, principles and development*, edited by W. Brown (Clarendon Press, Oxford, 1996), pp. 30–102.
[67] J.-P. Hansen and I. R. McDonald, *Theory of Simple Liquids*, 2nd ed. (Academic Press, London, 1986).

TABLES

f_1	f_2	N	λ
3	5	100	0.511
5	10	100	0.643
5	18	100	0.667
10	18	50	0.675
10	30	50	0.673
10	50	50	0.692
18	30	50	0.696
18	50	50	0.668
30	50	50	0.714

TABLE I. List of the simulated f_1-f_2-combinations and the corresponding results for $\lambda = \sigma/(R_{f_1} + R_{f_2})$. N is the associated monomer number per arm.

FIGURES

FIG. 1. Snapshot of two interacting star polymers with $f_1 = 18$ and $f_2 = 10$ arms.

FIG. 2. Reduced inverse force $k_BT/(R_{12}F_{f_1f_2})$ between the centers of two star polymers (for $f_1 = 10, f_2 = 50$ and $N = 50$) versus reduced distance r/R_{12}, where $R_{12} = (R_{f_1} + R_{f_2})/2$. The error bars were obtained by averaging over the results of 10 independent simulations. The dashed line is a linear regression of the data. The solid line is the theory from chapter II.

FIG. 3. Simulation results for the prefactor $\Theta_{f_1f_2}$ for $f_2 = 5 \ldots 50$ and $f_1 = 10$ fixed, in comparison to three different theoretical predictions.

FIG. 4. Simulation results (symbols) and theoretical results (lines) for the reduced effective force $R_{12}F_{f_1f_2}/k_BT$ versus reduced distance $(r - 2R^{(d)})/R_{12}$.

FIG. 5. Logarithm of the reduced force, $\ln(R_{12}F_{f_1f_2}/k_BT)$, versus reduced distance, $(r - 2R^{(d)})/R_{12}$, for $f_1 = 10, f_2 = 18$ and $N = 50$. The error bars were obtained by averaging over the results of 10 independent simulations.

FIG. 6. (a) Radial distribution function $g(r)$ and (b) center-to-center structure factor $S(k)$ for polydisperse star polymers in the fluid state. In the MC simulations, the average arm number has been chosen as $\bar{f} = 32$, the mean packing fraction as $\bar{\eta} = 0.5$. Polydispersities p as indicated in the figure.

FIG. 7. (a) Radial distribution function $g(r)$ and (b) center-to-center structure factor $S(k)$ for $\bar{f} = 40$, $\bar{\eta} = 0.5$. Polydispersities p as indicated in the figure.

von Ferber et al., Fig 1

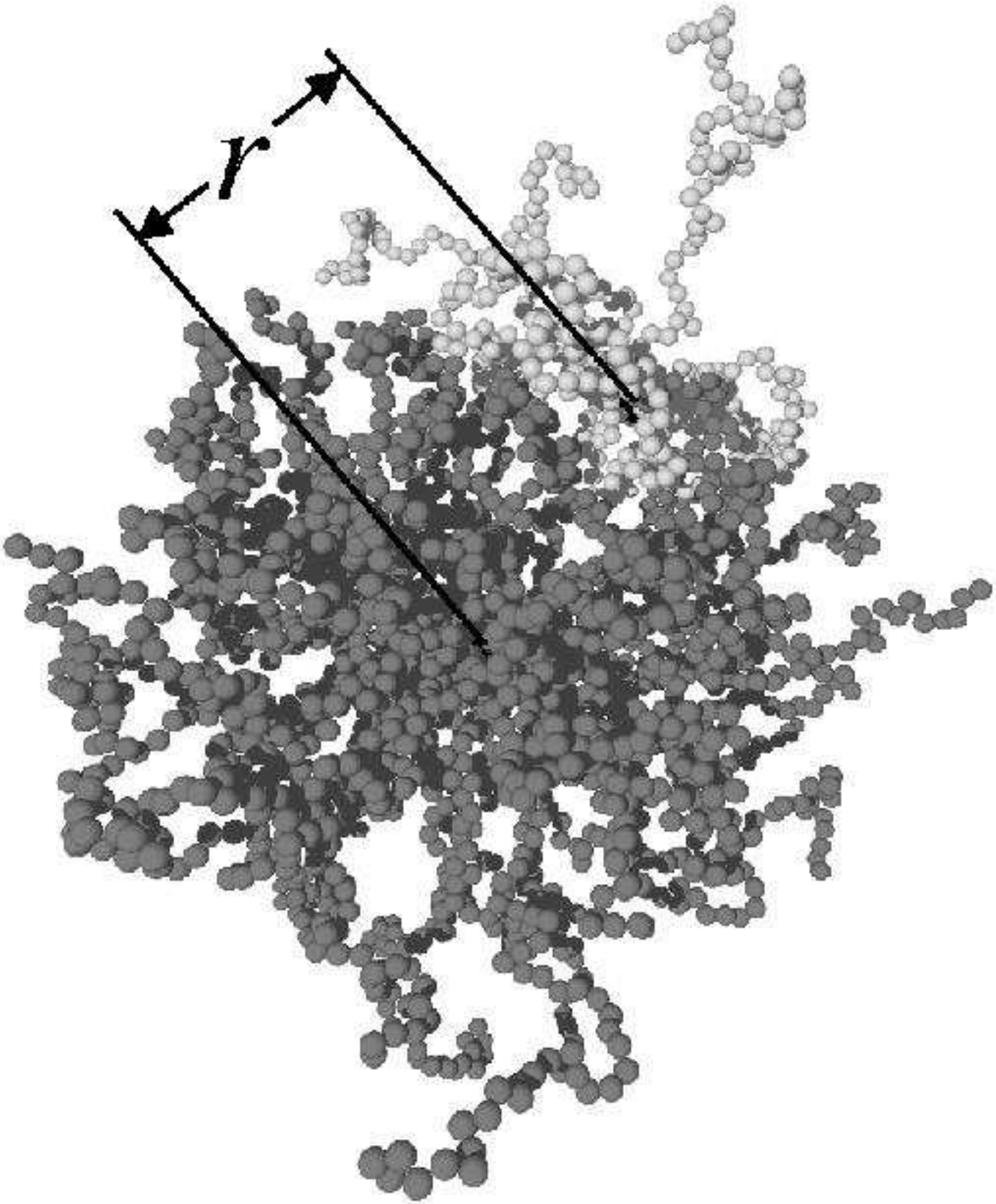

von Ferber et al., Fig. 2

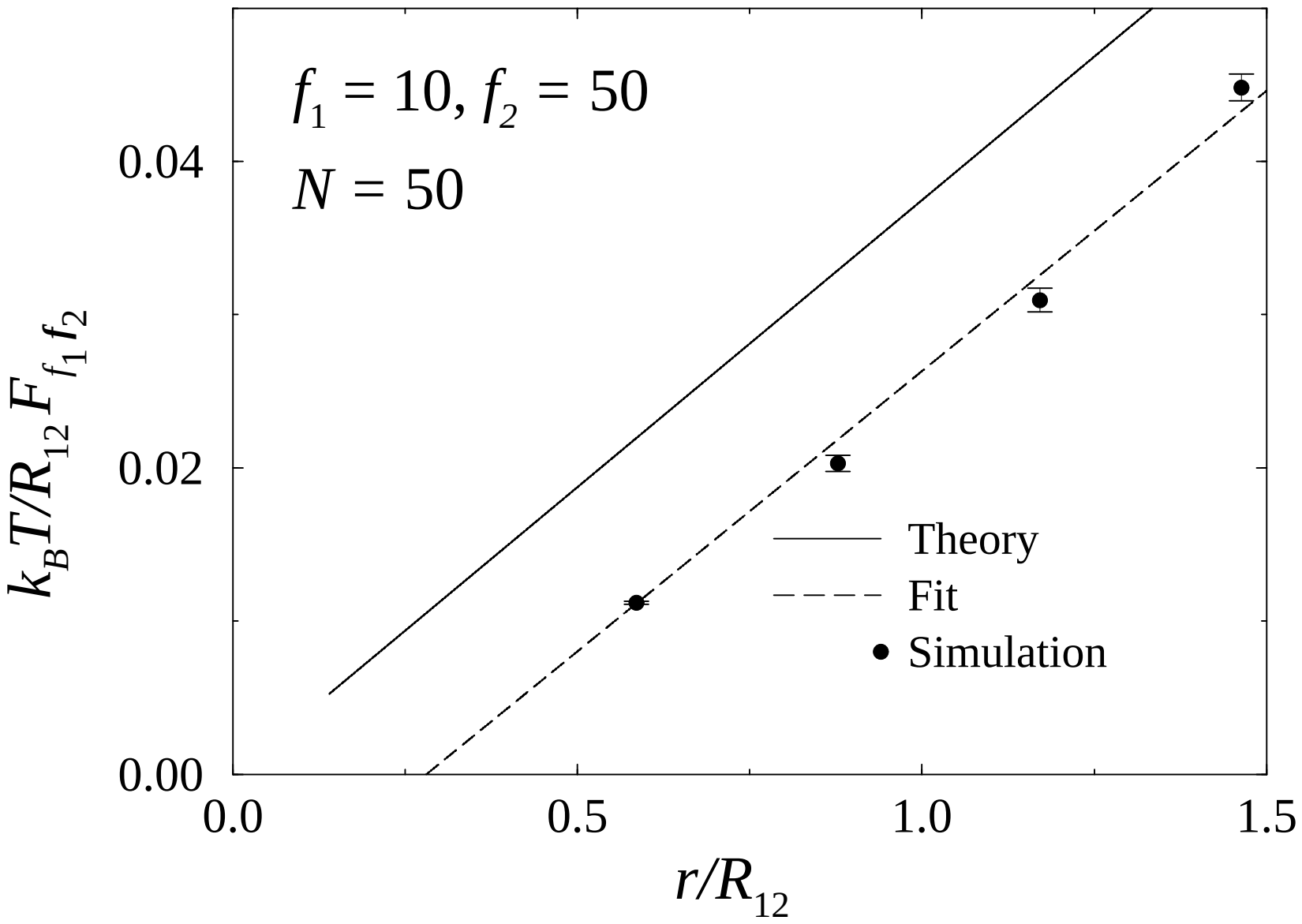

von Ferber et al., Fig. 3

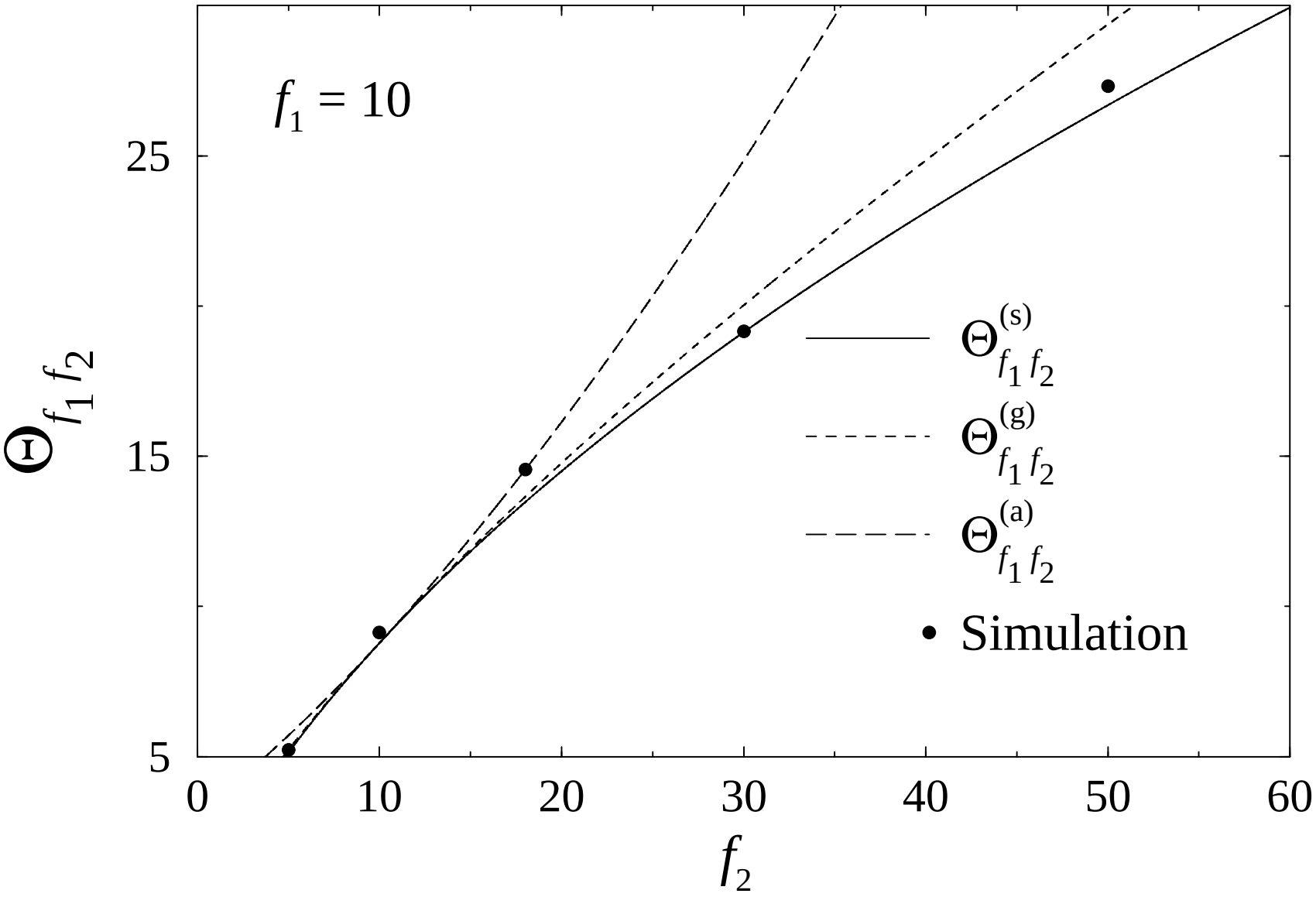

von Ferber et al., Fig. 4

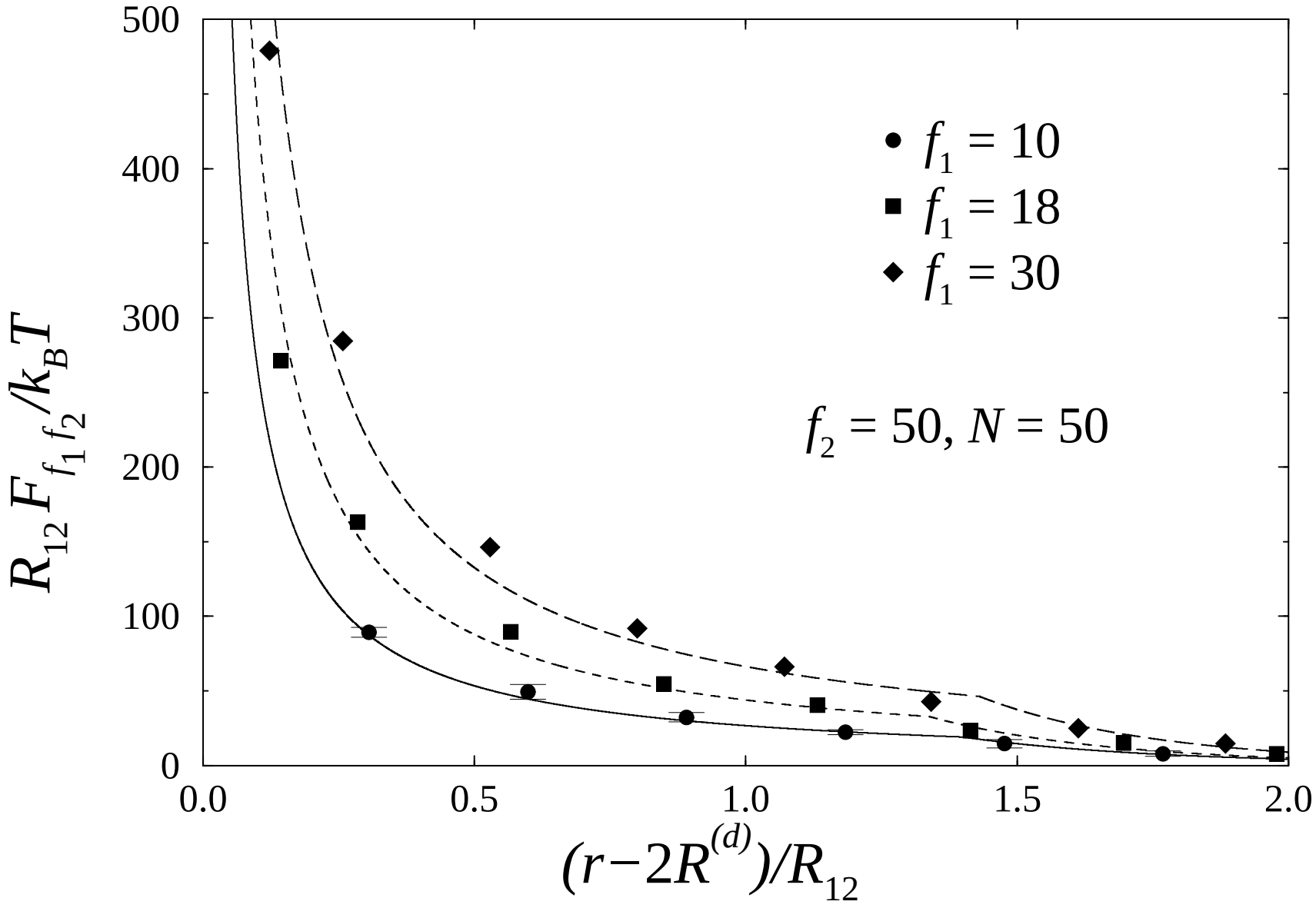

von Ferber et al., Fig. 5

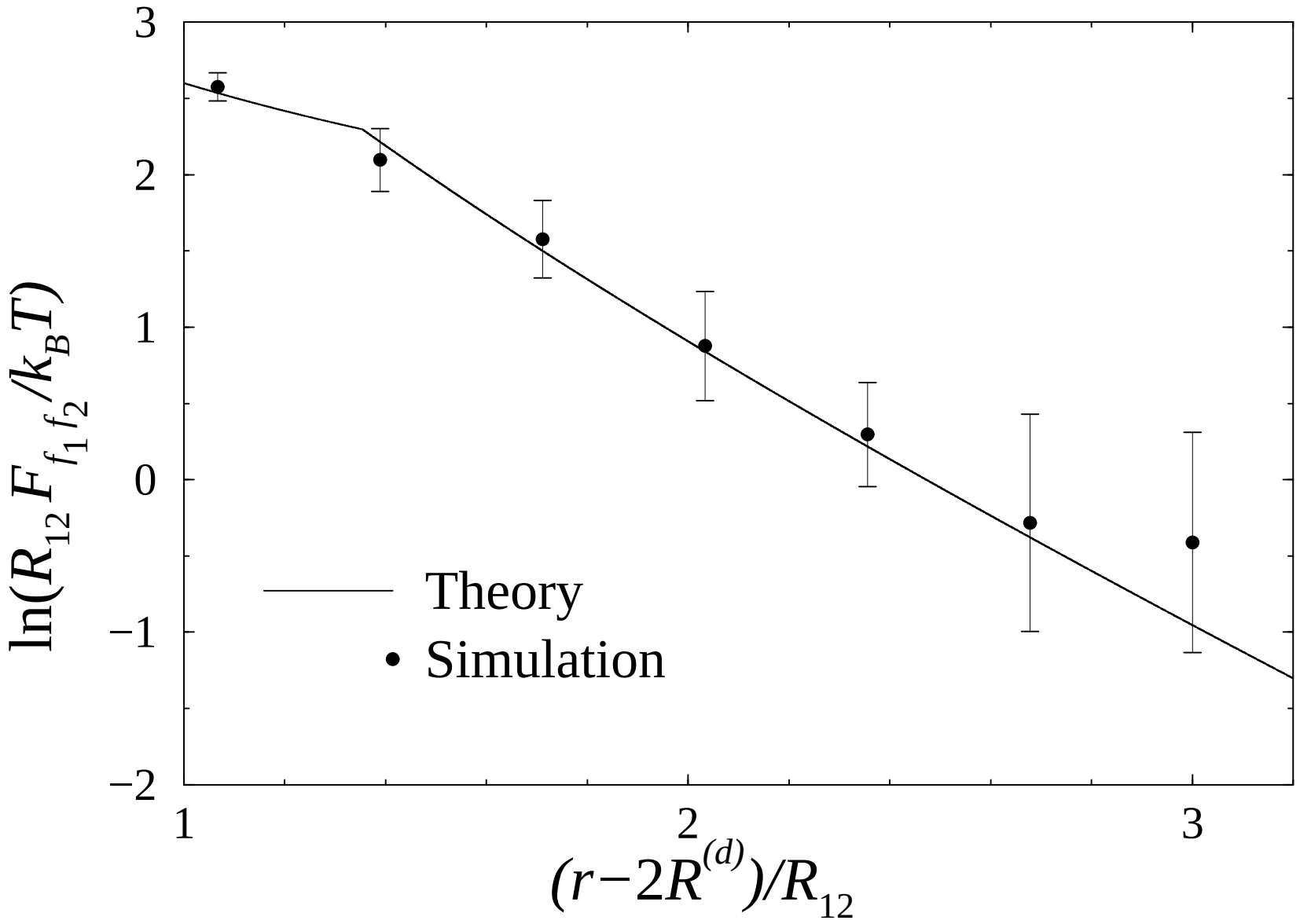

von Ferber et al., Fig. 6 a

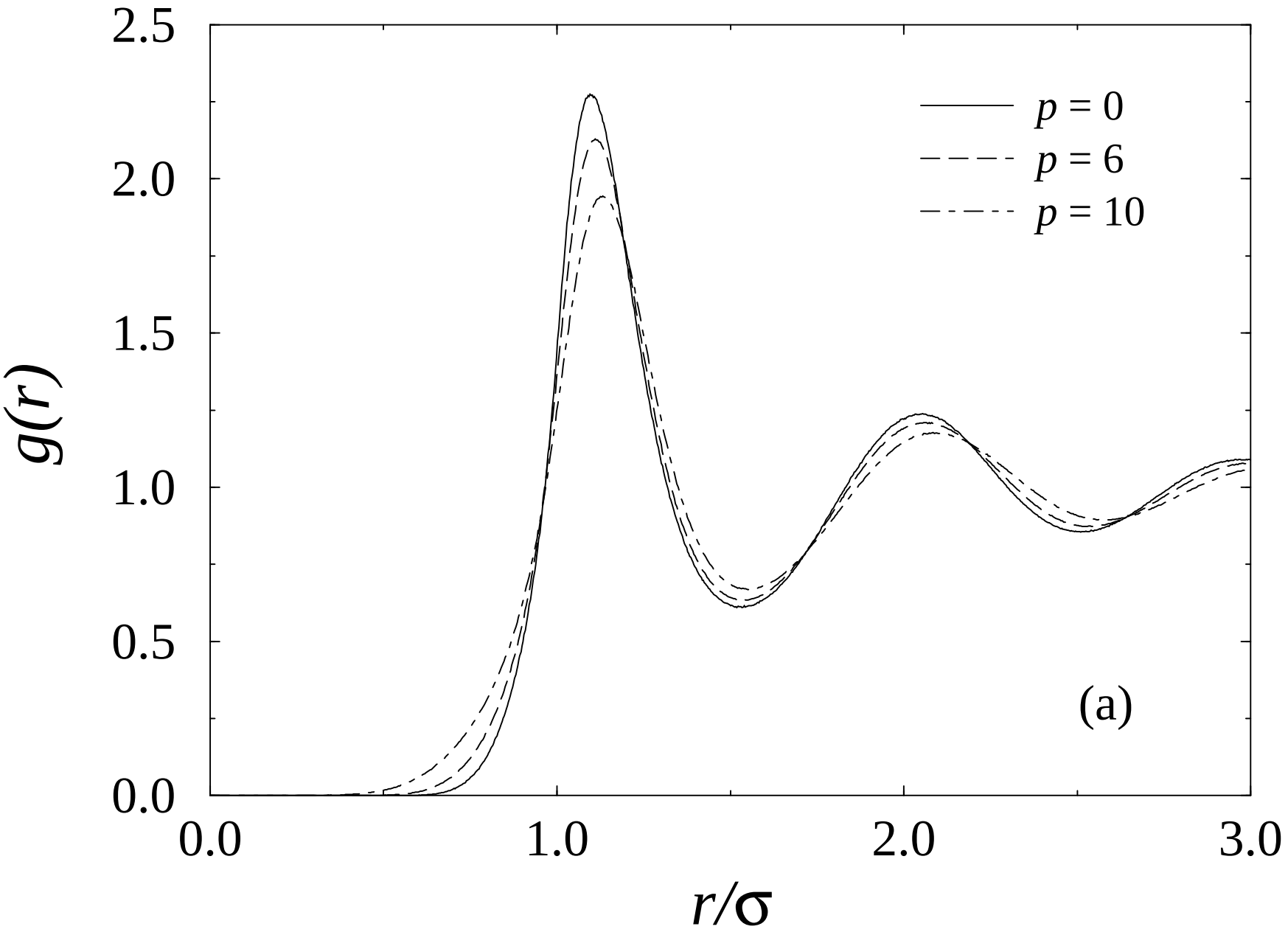

von Ferber et al., Fig. 6 b

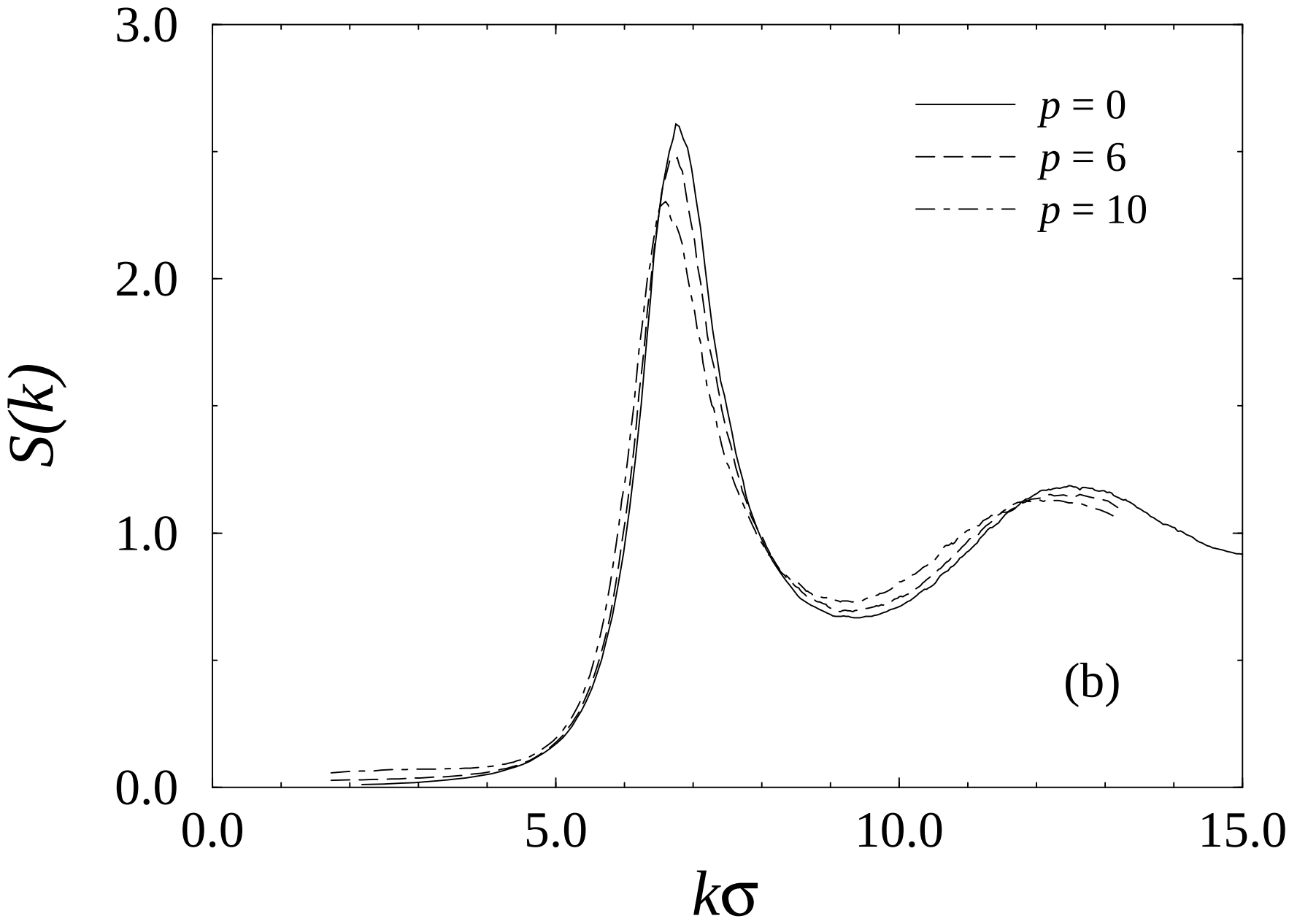

von Ferber et al., Fig. 7 a

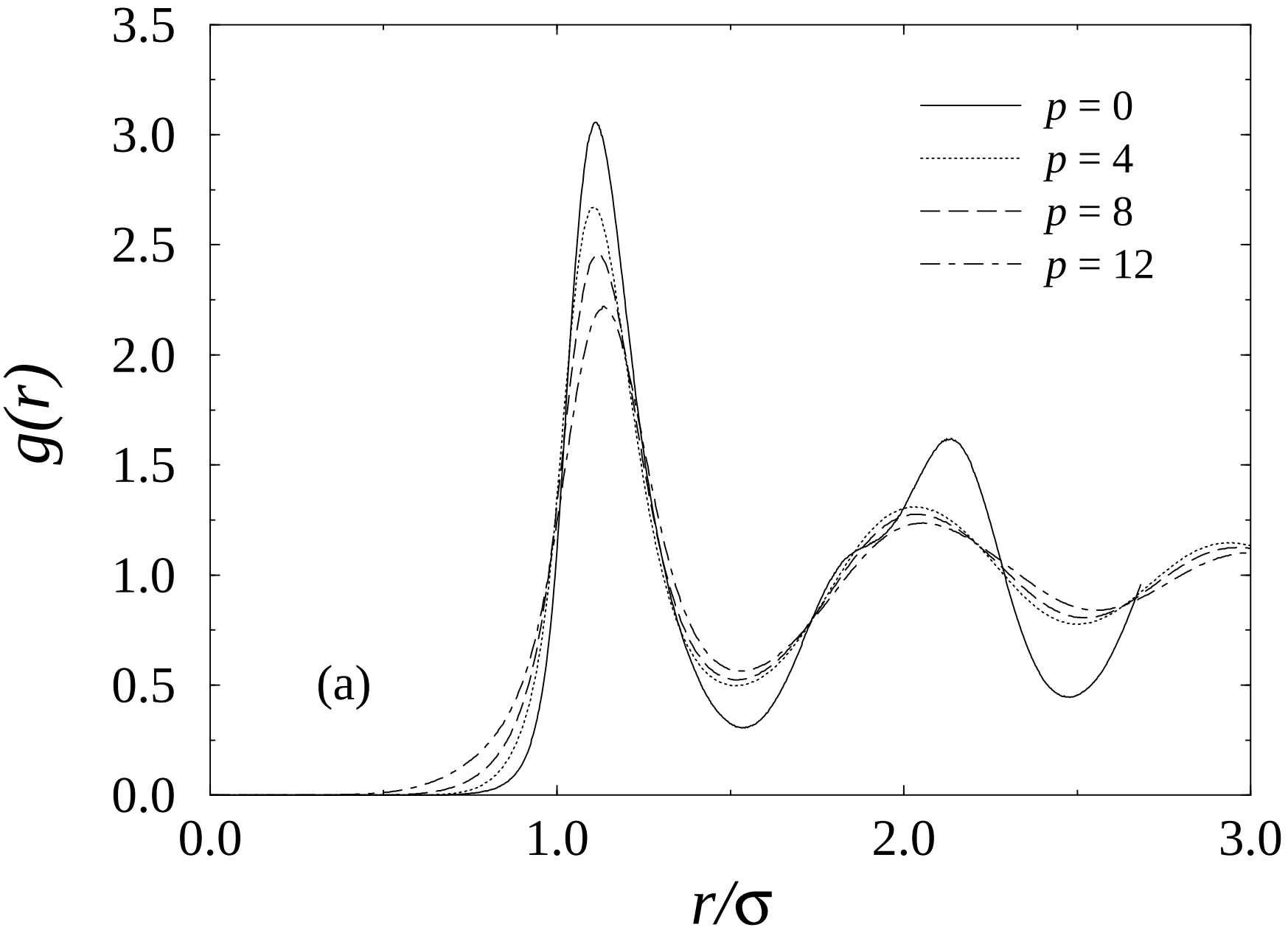

von Ferber et al., Fig. 7 b